SCIEPublish

Article

Material Analysis of CNT's as Conductive Additive for NMC Lithium-Ion Polymer Batteries Cathode Electrode

Fidelis Nwabunike Okonkwo [1,*], Solomon Chuka Nwigbo [1] and Anthony Chika Okonkwo [2]

[1] Mechanical Engineering Department, Faculty of Engineering, Nnamdi Azikiwe University, Awka 420007, Nigeria; sc.nwigbo@unizik.edu.ng (S.C.N.)

[2] Chemical Engineering Department, Faculty of Engineering, Nnamdi Azikiwe University, Awka 420007, Nigeria; chika.okonkwo@unizik.edu.ng (A.C.O.)

* Corresponding author. E-mail: fidelisokonkwo78@gmail.com (F.N.O.)

Received: 15 September 2025; Accepted: 15 October 2025; Available online: 29 October 2025

ABSTRACT: Carbon nanotubes (CNTs) are promising conductive additives for lithium-ion polymer (LiPo) batteries. The performance of lithium metal oxide cathodes is highly dependent on the properties of the conductive carbon additive. This study investigates the advantages of CNTs over conventional carbon black for this application. Material properties, including hardness, tensile strength, thermal conductivity, and electrical resistivity, were analyzed and compared using Ansys Granta (CES EduPack 2024 R2) software. The results demonstrate that CNTs are superior in tensile strength (110 MPa), hardness (50 HV), and thermal conductivity (210 W/m·°C). These properties enhance the mechanical integrity of the CNT-based cathode composite, leading to improved battery performance. Furthermore, the electrochemical behavior of CNT/$LiNi_{0.5}Co_{0.2}Mn_{0.3}O_2$ composite cathodes was investigated, focusing on the carbon precursor (methane *vs.* natural gas) and CNT diameter. At a current rate of 3 °C, multi-walled carbon nanotubes (MWCNTs) derived from methane delivered a specific capacity 20 mAh/g higher than those derived from natural gas. This indicates that methane-derived MWCNTs exhibit superior electrochemical performance, which is attributed to reduced polarization and a higher discharge potential. The study also revealed that MWCNTs with a smaller diameter (30–50 nm) performed better at high charge/discharge rates, owing to a higher number of primary particles per unit mass. This analysis aids in understanding material selection and its implications for battery design and lifecycle. The findings serve as a reference for future research exploring the use of CNTs in advanced battery materials.

Keywords: Lithium-ion polymer battery; $LiNi_{0.5}Co_{0.2}Mn_{0.3}O_2$ cathode; Carbon nanotubes; Multi-walled carbon nanotubes; Electrochemical performance

1. Introduction

Lithium-ion polymer (LiPo) batteries have emerged as promising rechargeable energy sources for electric vehicles and portable electronics [1–3]. As illustrated in Figure 1, a LiPo battery is a composite system whose operation depends on the interaction of its constituent components. The standard configuration includes a cathode and an anode, typically composed of lithium transition metal oxides and carbonaceous materials, respectively [4–6]. Carbon-based conductive additives are incorporated to enhance the electronic conductivity of these electrodes. Current collectors facilitate electron transfer between the electrodes and the external circuit while providing mechanical support to the active layers. A polymer-based binder integrates the electrode components and bonds the active material to the current collector [7]. A porous separator physically isolates the electrodes, preventing electrical short circuits while permitting ionic charge transport [8–10].

https://doi.org/10.70322/spe.2025.10011

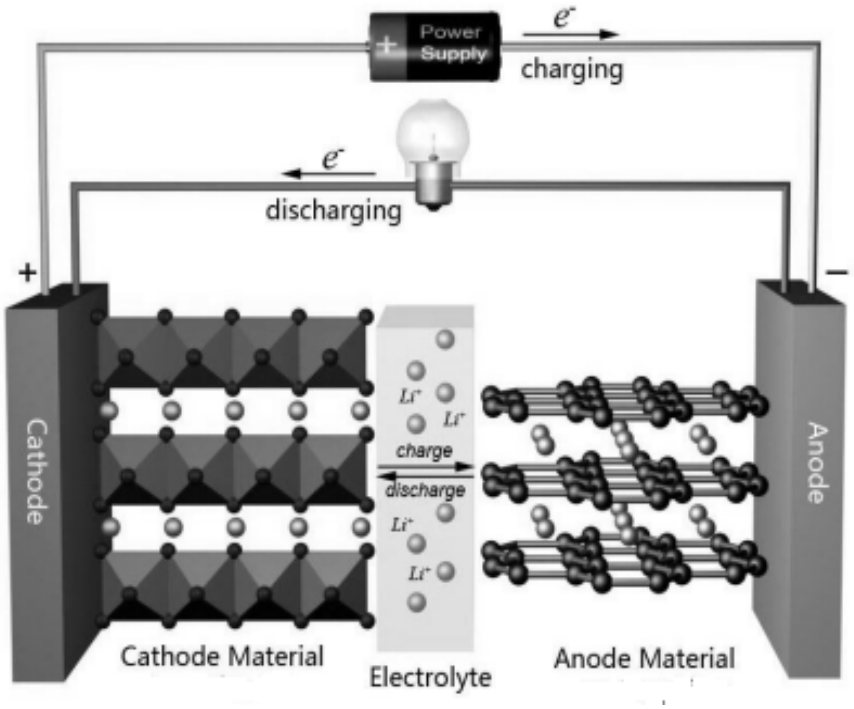

Figure 1. Charge and discharge operation of Lithium-ion battery [11].

The limited cycling durability of electrodes composed solely of cathode active material is primarily attributed to the low intrinsic electronic conductivity of transition metal oxides [12,13]. Chen et al. have noted that strategies to enhance electrode conductivity through bulk and surface modifications of the active material have proven impractical [14]. In contrast, incorporating carbon black into the composite electrode dramatically enhances its overall conductivity, surpassing the bulk conductivity of the active material by more than twentyfold [15]. The conductive additive plays a critical role in bolstering the electrode's structural stability, electrochemical performance, and electronic conductivity [16,17]. Achieving an optimal balance between the binder and additive proportions is essential for producing a composite electrode with high conductivity and mechanical strength [16]. This conductive network establishes a low-resistance pathway for electron flow between active material particles and the current collector. This facilitation of rapid electron transport mitigates polarization effects and improves active material utilization. Furthermore, the conductive additive can act as an electrolyte reservoir, fostering closer proximity between the host material and Li^+ ions, further enhancing utilization [8,18,19]. Carbon-based materials are particularly promising as conductive additives for the positive electrode in Li-ion batteries due to their high thermal and electronic conductivity, cost-effectiveness, low toxicity, low density, and chemical inertness [20–31].

Carbon nanotubes (CNTs) have garnered significant interest across numerous fields due to their exceptional electrical, thermal, mechanical, and structural properties. Their structure consists of carbon atoms arranged in a folded, hexagonal honeycomb lattice. This arrangement results in high electrical conductivity because each carbon atom uses only three of its four valence electrons to form covalent bonds, leaving the fourth electron delocalized and free to conduct electricity. The properties of CNTs—such as electrical conductivity, mechanical strength, and chemical reactivity—are not intrinsic constants but are highly dependent on critical parameters, including tube diameter, synthesis precursor, and weight fraction. For instance, the average diameter of CNTs, which typically ranges from 10 to 250 nm, profoundly influences their characteristics and potential applications. A comprehensive understanding of these structure-property relationships is essential for tailoring CNTs for specific uses, such as optimizing their performance as conductive additives in lithium-ion battery cathodes.

The structural features of carbon nanotubes (CNTs) are commonly characterized using a suite of techniques, including thermogravimetric analysis (TGA), Fourier transform infrared spectroscopy (FTIR), transmission electron microscopy (TEM), X-ray diffraction (XRD), scanning electron microscopy (SEM), and X-ray photoelectron spectroscopy (XPS), among others. Each method has inherent constraints, and no single technique can comprehensively examine all CNT characteristics. XRD and SEM are widely used due to their relatively fewer limitations. XRD, in particular, is distinguished by its ability to elucidate key physicochemical properties of CNTs, such as crystallinity, phase composition, and interlayer spacing [32]. Figure 2 illustrates the hexagonal carbon structure of CNTs and a model

of a multi-walled carbon nanotube (MWCNT). MWCNTs are particularly advantageous as conductive additives due to their exceptional electronic properties. CNTs form a superior electron transfer network when integrated into a nickel-enriched cathode material. This well-structured network enhances cycling performance by facilitating stable phase transitions and maintaining a consistent average voltage during charge/discharge cycles. Furthermore, the CNT-based electrode demonstrates improved electrochemical properties at high current densities. The pervasive conductive network mitigates polarization by reducing the cell's internal resistance, thereby enhancing performance under demanding conditions.

Carbon black (CB) is a particulate form of elemental carbon produced through the vapor-phase pyrolysis and partial combustion of hydrocarbons. It is classified by its production method—such as acetylene black, furnace black, and thermal black—which dictates its primary particle size distribution and the degree of particle aggregation and agglomeration. In commercial CBs, aggregate diameters typically range from 10 to 500 nm, while larger agglomerates can span several micrometers. Carbon black must be thoroughly characterised before being incorporated into valuable applications like the positive electrode of $LiNi_{0.5}Co_{0.2}Mn_{0.3}O_2$ batteries. Analytical techniques are essential to determine its material properties, enabling reliable prediction and simulation of its electrochemical performance in lithium-ion polymer batteries [33].

The Ansys Granta software (CES EduPack 2024 R2) suite provides a unique advantage for comparing conductive additives by facilitating the visualization of material properties through performance charts and data. This capability offers a clear, data-driven rationale for material selection. Granta establishes a systematic framework for managing materials data, which aids in implementing intelligent selection algorithms and fosters innovation in battery material design—all of which are of significant technical and commercial importance. Within the battery industry, Granta plays a critical role in materials information management, including the evaluation of life cycle impacts and potential hazards associated with substances of concern. The software offers extensive databases of commonly employed materials and manufacturing processes across categories such as polymers, metals, ceramics, and composites. Each database contains numerous datasets, with a focus on bulk material properties, joining techniques, and shaping processes. The underlying philosophy for this approach is grounded in Ashby's methodology, which states that material selection must be based on the component's function, the material's properties and availability, and the manufacturing process used to create the final shape [34–36].

A combination of technical, economic, and environmental criteria guides the selection of electrode materials for lithium-ion batteries. Ideal materials should be inherently available, low-cost, not in high demand from competing industries, and environmentally benign throughout their processing, use, and end-of-life recycling. From a technical perspective, electrode materials must provide a high theoretical capacity, a function of the molar weight and the number of electrons transferred per formula unit during the redox reaction. This is equivalent to the number of Li^+ ions the host lattice can reversibly intercalate. Transition metal oxides are particularly advantageous as cathode materials because their variable valence states provide multiple sites for redox reactions, enabling high capacity. Common cathode active materials include lithium cobalt oxide ($LiCoO_2$), lithium manganese oxide ($LiMn_2O_4$), lithium iron phosphate ($LiFePO_4$), and lithium nickel manganese cobalt oxide ($LiNiMnCoO_2$ or NMC). These materials offer different trade-offs in energy density, thermal stability, and cost. Research indicates that the key to achieving a high-rate capability lies in using low-valent transition metal ions and ensuring low structural strain during lithium (de)intercalation. Consequently, layered metal oxides, particularly NMC compositions, are among the most effective systems for applications requiring high power, such as fast charging. The formulation of the composite electrode is equally critical. While the polymer binder is an inactive component, constituting only 2–5% of the commercial electrode mass, it is crucial for forming a uniform electrode film, enhancing high-rate performance, and ensuring long-term cycle stability [37]. Theoretical simulations suggest that optimal cathode performance is achieved with a high active material content (≥90%) and a polymer binder-to-conductive additive ratio of less than 4 [38]. Ultimately, the final selection criteria and electrode formulation depend on the specific battery type and its intended application.

This research presents a comprehensive analysis of carbon nanotubes (CNTs) as conductive additives for lithium-ion battery cathodes, utilizing Ansys Granta software (CES EduPack 2024 R2) for material property evaluation. The study directly compares CNTs and carbon black based on key properties, including hardness, tensile strength, thermal conductivity, and electrical resistivity. Furthermore, the electrochemical performance of CNT/$LiNi_{0.5}Co_{0.2}Mn_{0.3}O_2$ (NMC532) composite cathodes is investigated, with a specific focus on the influence of CNT carbon precursor (methane *vs.* natural gas) and CNT diameter. The primary aim of this work is to understand material selection by elucidating its impact on performance and incorporating a lifecycle perspective during the battery design and development stages. The manuscript is structured into four main sections: Introduction, Materials and Methods (including experimental details), Results and Discussion, and Conclusions.

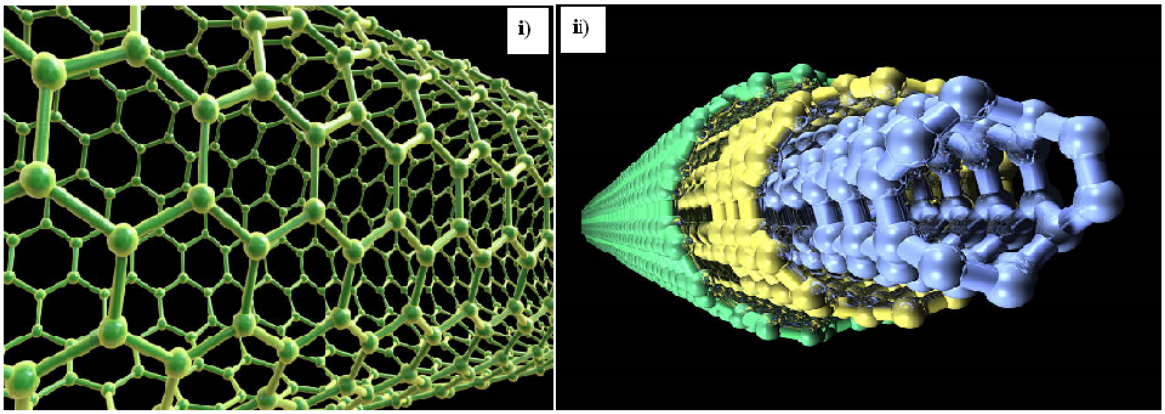

Figure 2. (**i**) 3D illustration of carbon nanotubes and (**ii**) a model of a multi-walled carbon nanotube; featuring several concentric cylindrical lattices of carbon atoms providing exceptional improvement of cathode electrode performance and well conducting network.

2. Materials and Methods

This study utilized a lithium metal oxide cathode in a pouch cell (BZ605060), incorporating CNT/$LiNi_{0.5}Co_{0.2}Mn_{0.3}O_2$ conductive additives. The cathode formulations featured varying concentrations of active material and binder, as detailed in Table 1.

The material properties of carbon nanotubes (CNTs) and carbon black (CB) were compared using the (CES EduPack 2024 R2) in its advanced mode. The software provided detailed data for both materials across multiple categories, including general, mechanical, electrical, and thermal properties. Specific properties analyzed were tensile strength and hardness. Bubble charts were generated for the two conductive additives to facilitate a direct visual and numerical comparison, streamlining the analysis and enhancing the understanding of their characteristics. For instance, Figure 3 presents a bubble chart plotting Electrical Resistivity (μΩ·cm) against Hardness (HV), created as a default log-log plot within the software.

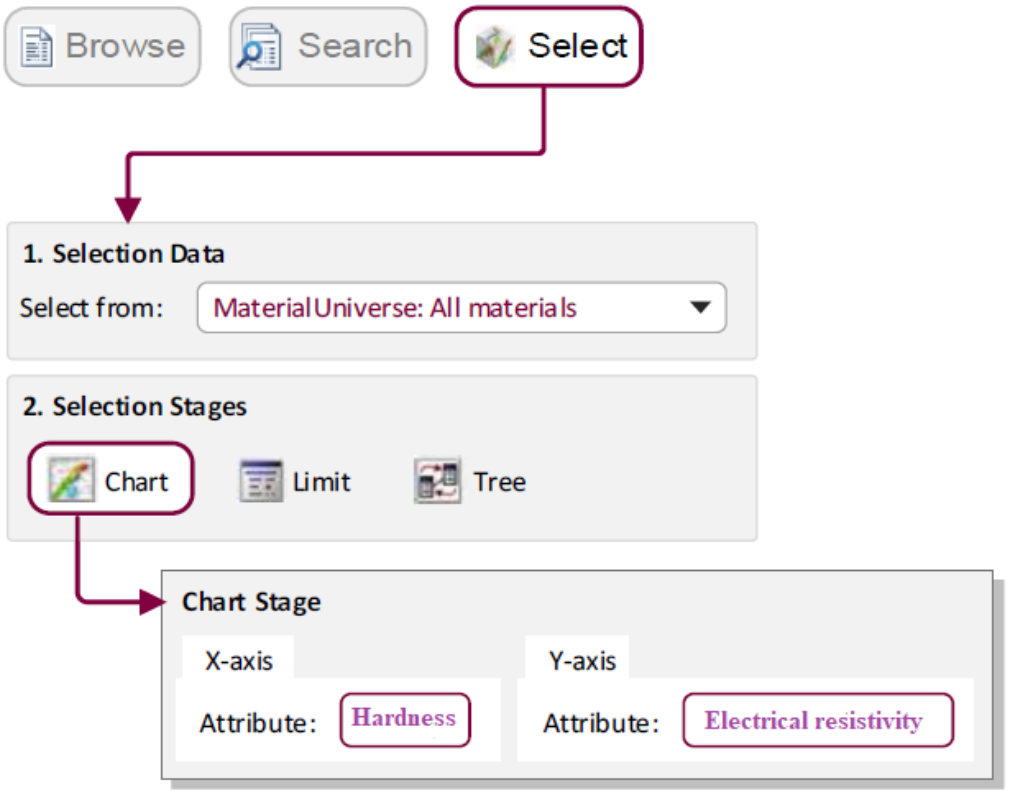

Figure 3. A bubble chart plot process for Electrical resistivity against Hardness.

Table 1. The composition and characteristics of the cathode electrode.

No.	Item	Parameter	Note
1.	Nickel	0.5%	Percentage concentration of Ni
2.	Manganese	0.3%	Percentage concentration of Mn
3.	Cobalt	0.2%	Percentage concentration of Co
4.	$Li(Ni_{0.5}Co_{0.2}Mn_{0.3})O_2$	93%	Percentage weight of active material (NMC)
5.	Binder	3.5%	Percentage weight of binder
6.	$(CNTs/LiNi_5Co_2Mn_3O_2)$	3.5%	Percentage weight of conductive additive
7.	Current collector	10 μm	Thickness of Aluminium/Copper foil
8.	Electrode porosity	33%	Positive electrode
9.	Coating	8 μm	Coating thickness
10.	Loading (cathode)	3.20 mAh/cm^2	
11.	Loading (anode)	3.53 mAh/cm^2	

2.1. Experimental

Multi-walled carbon nanotubes (MWCNTs) with an average diameter of 150–250 nm were acquired from Sigma-Aldrich (St. Louis, MO, USA) and used as received. The crystalline structure was characterized by X-ray diffraction (XRD; Rigaku Miniflex6000, C-THERM, Brunswick, NB, Canada) using Cu Kα radiation at 45 kV and 45 mA. Morphology and dimensions were assessed using a scanning electron microscope (SEM; Phenom Prox, Thermo Fisher Scientific, Breda, The Netherlands). Electrical resistance was measured with a four-point probe system (ZZ Universal 64 Full-Channel Resistivity Meter, ZZ Resistivity Imaging Pty. Ltd., Maylands Adelaide, South Australia). The cathode was fabricated from a slurry containing 93 wt% $LiNi_{0.5}Co_{0.2}Mn_{0.3}O_2$ (NMC532, SN2G, Soundon New Energy Co., Ltd., Shanghai, China) as the active material, 3.5 wt% polyvinylidene difluoride (PVDF-900 HSV, France) as the binder, and 3.5 wt% MWCNTs (Soundon New Energy Co., Ltd., Shanghai, China) as the conductive additive. The anode slurry consisted of 96 wt% artificial graphite (MAG-507, Shenzhen Sinuo Industrial Development Co., Ltd., Shenzhen, China), 2.5 wt% PVDF, and 1.5 wt% Super P-Li carbon black. Based on an N-methyl-2-pyrrolidone (NMP) solvent, both slurries were coated onto current collectors—the cathode onto 10 μm thick aluminum foil and the anode onto 10 μm thick copper foil. The coated electrodes were vacuum-dried overnight at 100 °C and subsequently calendared to enhance particle contact. The final electrode loadings were 3.20 mAh/cm^2 for the cathode and 3.53 mAh/cm^2 for the anode.

Pouch-type lithium-ion cells with a nominal capacity of 3000 mAh were assembled (Model 605060, Benzo Energy Technology Co., Ltd., DongGuan, China; 6 mm thickness × 50 mm width × 60 mm height; 38 g weight). Each cell incorporated the prepared NMC cathode, graphite anode, and a polypropylene (PP) separator. The electrolyte consisted of 1 M $LiPF_6$ in a mixture of ethylene carbonate (EC), diethyl carbonate (DEC), and ethyl methyl carbonate (EMC) (1:1:1 by volume), with 2% propylene carbonate (PC) and 1% vinylene carbonate (VC) as additives. Cell lamination was performed in a dry room 25 min after electrolyte injection. Electrochemical performance was evaluated using a multi-channel battery tester (HT3563A, Hopetech, Changzhou, China). All cycling tests were carried out within a voltage window of 2.8 V to 4.3 V (*vs.* Li^+/Li). The rate capability was assessed at a 3.0C discharge rate after an initial formation process of 6 cycles.

2.2. Electrochemical Properties Evaluation of the Cathode Materials

The electrochemical behavior of the lithium insertion materials was evaluated using galvanostatic charge/discharge testing. The $LiNi_{0.5}Co_{0.2}Mn_{0.3}O_2$ (NMC) cathode functions by electrochemically extracting and inserting Li^+ ions through a reversible redox process. The cells were initially cycled at a low current rate of 0.01C to characterize the materials under near-equilibrium conditions. The rate capability and cyclability were subsequently assessed at a higher current rate of 0.2C for approximately six charge/discharge cycles. The charging protocol consisted of a constant current (CC) step followed by a constant voltage (CV) step. During the CV step, the cell was held at 4.2 V while the current was monitored; the current decayed over time as the electrode approached full charge. Once the current decreased to a predetermined cutoff, the cell was allowed to rest at open circuit for 30 min before a constant current discharge. The high coulombic efficiency and stable voltage profiles observed in these tests indicate that the Li^+ insertion/extraction reaction is highly reversible with minimal side reactions.

3. Results and Discussion

The property comparisons between carbon nanotubes (CNTs) and carbon black (CB) are summarized in Figures 4–6. Figure 4 plots electrical resistivity against hardness, revealing that CNTs possess a greater hardness of 50 HV than 40 HV for carbon black. This enhanced mechanical robustness in CNTs originates from their seamless hexagonal lattice of sp^2-hybridized carbon atoms, forming a covalently bonded structure. In a composite electrode, this hardness contributes to a more rigid scaffold that can help maintain structural integrity over multiple charge/discharge cycles, thereby improving capacity retention.

Figure 5 compares electrical resistivity with thermal conductivity. A key distinction is observed: CNTs exhibit a significantly higher thermal conductivity (210 W/m·°C) than carbon black (30 W/m·°C). This property is critical for battery safety and performance, as efficient heat dissipation mitigates hotspots during high-rate operation. The high thermal conductivity in CNTs arises from the efficient propagation of phonons along their rigid, one-dimensional structure.

Despite these mechanical and thermal properties differences, both materials show comparable electrical resistivity, approximately 5000–6000 μΩ·cm, confirming their primary function as effective conductive additives. However, the electrical conduction mechanism differs; in CNTs, electrical conductivity is facilitated by the delocalized π-electrons from the sp^2 carbon bonds, allowing for ballistic transport along the tube axis.

Figure 6 illustrates the contrast in tensile strength, with CNTs exhibiting a value of 110 MPa versus 15 MPa for carbon black. This order-of-magnitude difference is due to the strong covalent C-C bonds and the near-perfect, continuous structure of individual nanotubes, whereas carbon black consists of amorphous, particulate aggregates. The high tensile strength of CNTs contributes to a more durable conductive network within the composite electrode, which is less prone to mechanical degradation during cycling.

The combination of high tensile strength, hardness, and thermal conductivity—while maintaining low electrical resistivity—makes CNTs a superior conductive additive to carbon black, leading to enhanced rate capability and cycle stability in composite electrodes.

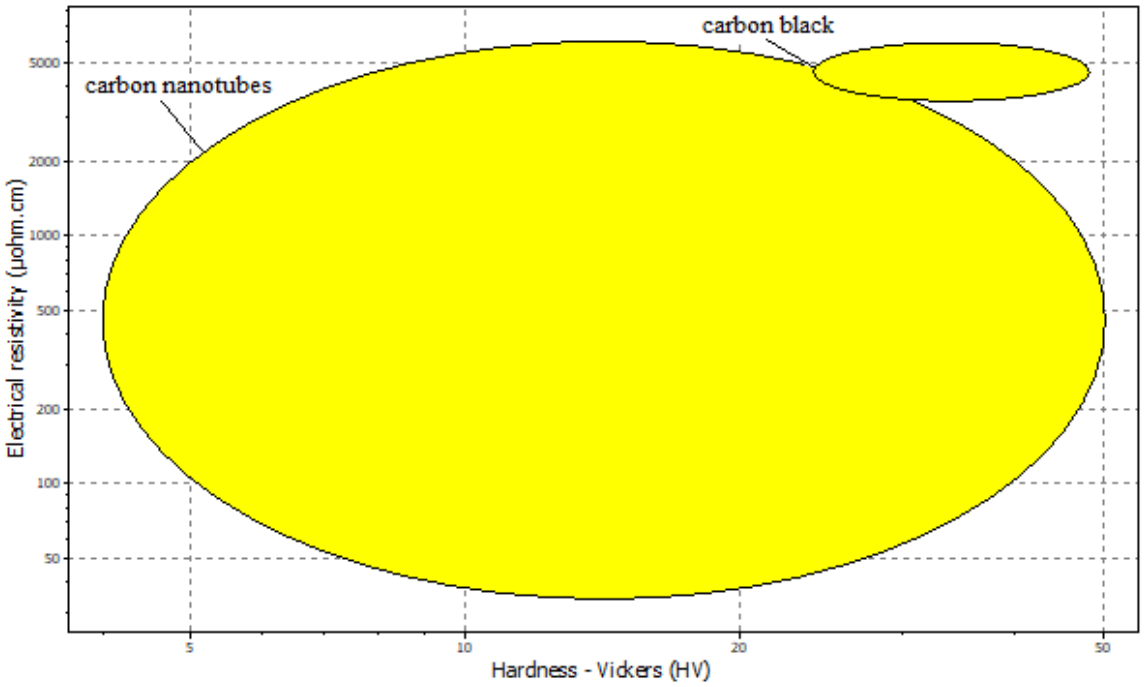

Figure 4. Chart of electrical resistivity against hardness for conductive material.

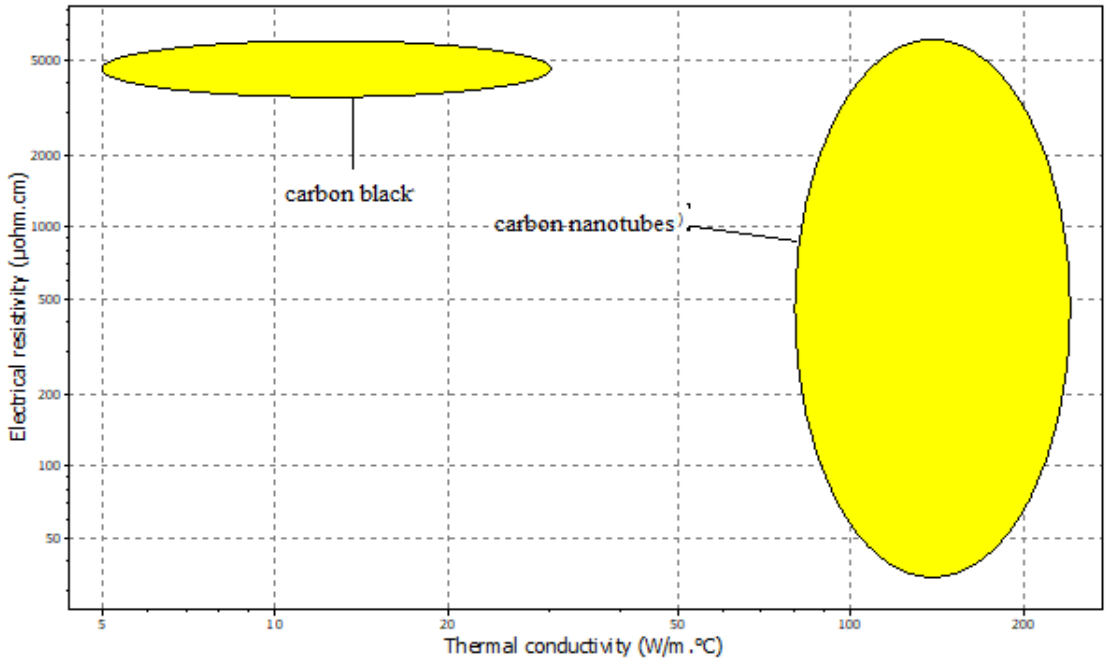

Figure 5. Chart of electrical resistivity against thermal conductivity for conductive material.

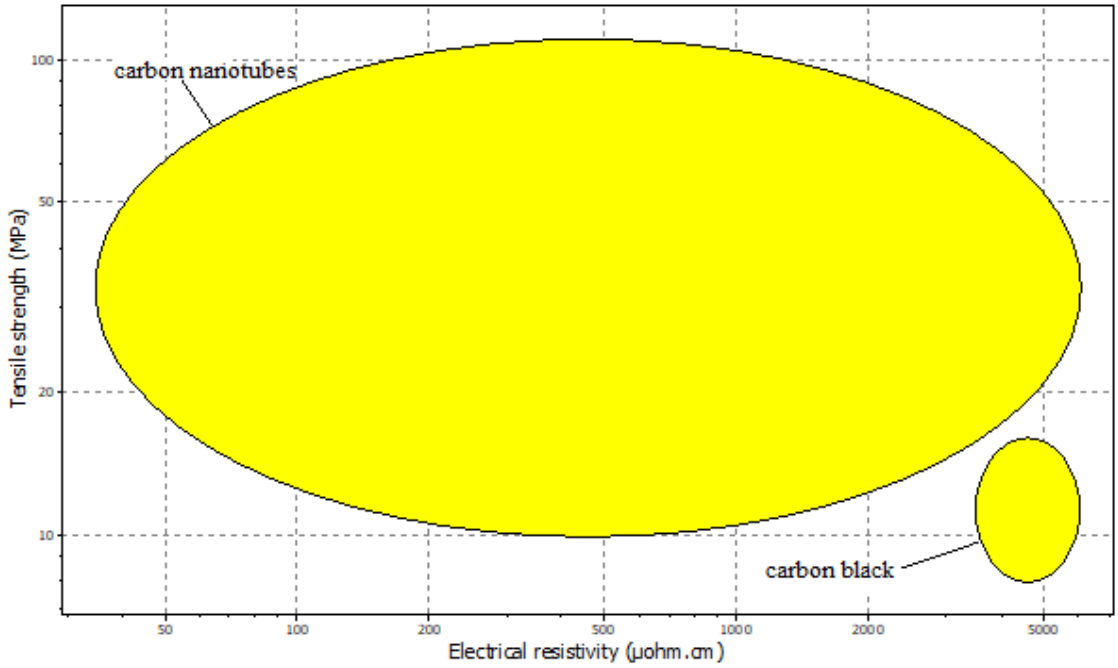

Figure 6. Chart of tensile strength against electrical resistivity for conductive material.

3.1. Carbon Nanotube Derivatives

The X-ray diffraction (XRD) pattern in Figure 7 reveals the structural characteristics of multi-walled carbon nanotubes (MWCNTs) synthesized using methane as the carbon precursor. The (002) diffraction peak, which corresponds to the interlayer spacing (d(002)), is a key indicator of graphitization quality. The d(002) spacing for the synthesized MWCNTs was calculated to be 0.3413 nm, which is very close to the value for highly ordered graphite (0.3373 nm). This close agreement indicates a high degree of crystallinity in the MWCNTs.

The scanning electron microscopy (SEM) images in Figure 8 illustrate the morphology of the CNTs derived from the two different carbon precursors, methane and natural gas. The MWCNTs exhibit a uniform tubular morphology with consistent diameters. Notably, the MWCNTs derived from methane (Figure 8i) display a smooth and pristine surface, suggesting a well-graphitized structure with minimal observable defects. The composite nanoparticles exhibit

excellent electro-catalytic activities with an electrochemically active surface area suggesting better performance when compared with natural gas.

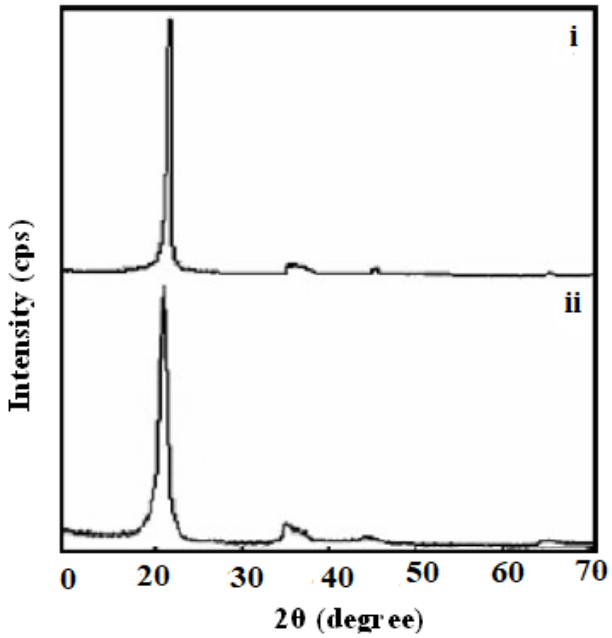

Figure 7. The XRD pattern of the CNT's prepared from methane, (**i**) and natural gas, (**ii**).

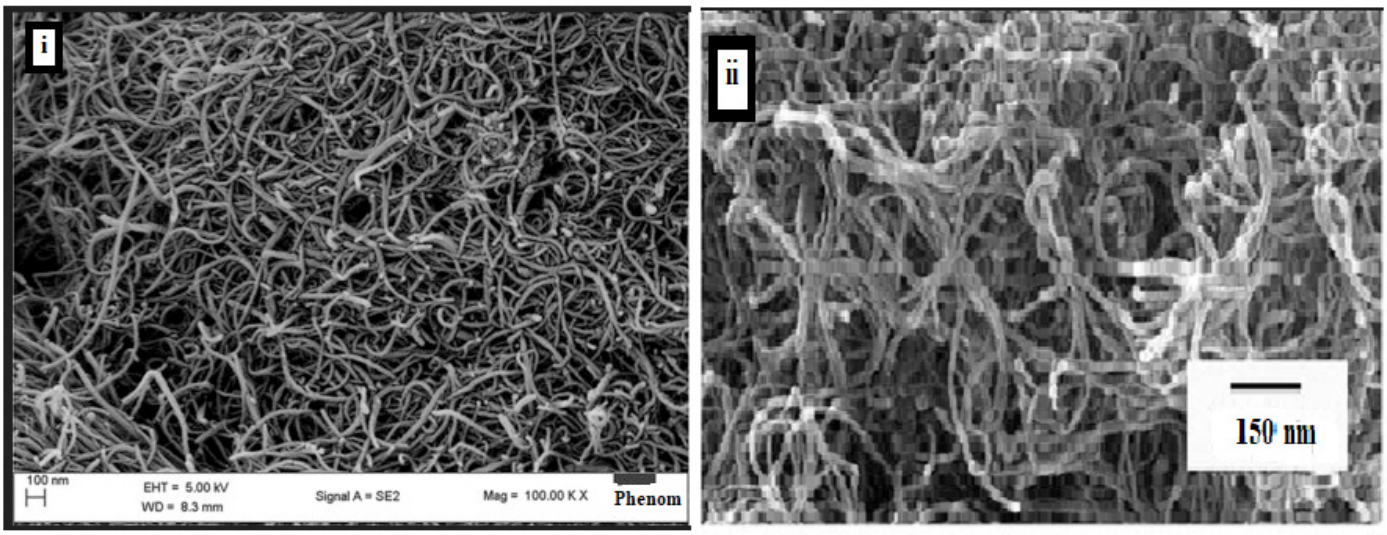

Figure 8. (**i**) SEM image of the carbon nanotubes in LiPo battery derived from methane and (**ii**) natural gas.

At low current rates, the two MWCNT/$LiNi_{0.5}Co_{0.2}Mn_{0.3}O_2$ composite cathodes exhibit nearly identical specific capacities. However, as shown in Figure 9, a significant divergence in discharge capacity emerges at higher current rates. Specifically, at 3.0C, the specific capacity difference between the cathode using methane-derived MWCNTs and the one using natural gas-derived MWCNTs widens to approximately 20 mAh/g.

The composite cathode incorporating methane-derived MWCNTs demonstrates superior rate performance. This enhancement is attributed to its lower internal resistance, which reduces polarization during high-rate discharge. The reduced polarization leads to a higher operating discharge potential, thereby increasing the specific capacity delivered by the cell. This effect is further illustrated in Figure 10, where the discharge curve for the superior cathode maintains a higher voltage plateau for a longer duration, especially as the discharge process nears completion. This results in a greater area under the voltage-capacity curve and a higher delivered specific capacity.

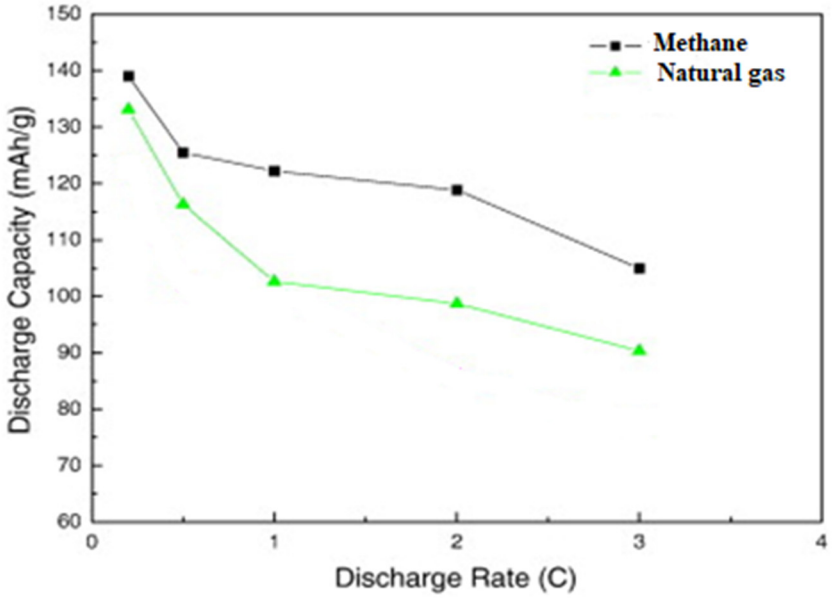

Figure 9. Initial discharge capacities and discharge rate of the CNT's prepared from methane and natural gas.

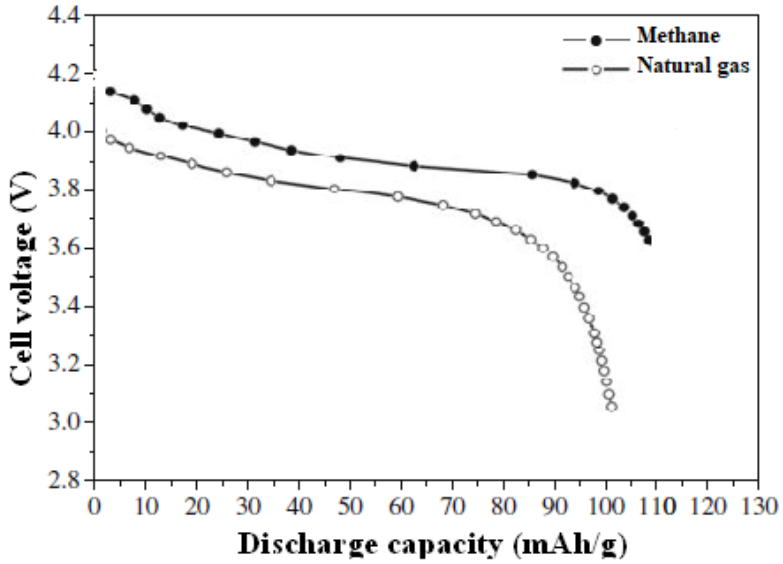

Figure 10. Initial discharge voltage profile of the CNT's prepared from methane and natural gas at 3.0C discharge rate.

3.2. Diameter Analysis

Figure 11 demonstrates that MWCNT/$LiNi_{0.5}Co_{0.2}Mn_{0.3}O_2$ cathodes with different MWCNT diameters exhibit similar discharge capacities at low current rates. However, a significant performance divergence emerges at higher rates. Cathodes incorporating MWCNTs with smaller diameters (30–50 nm) show a distinct advantage under these demanding conditions. For instance, at a charge/discharge rate of 3.0C, the specific capacity of the composite cathode with 30–50 nm MWCNTs is approximately 40 mAh/g higher than that of the cathode with 100–250 nm MWCNTs. This trend indicates that smaller-diameter MWCNTs significantly enhance the high-rate electrochemical performance of the composite cathode. This enhancement can be attributed to several factors. First, the smaller diameter reduces polarization by shortening the diffusion path for both electrons and Li^+ ions, thereby improving the kinetics of the redox reactions. Second, smaller-diameter MWCNTs possess a higher specific surface area, which maximizes the number of accessible charge transport channels and provides a more extensive conductive network. This lowers the overall contact resistance within the electrode, which is critical for maintaining performance at high current rates.

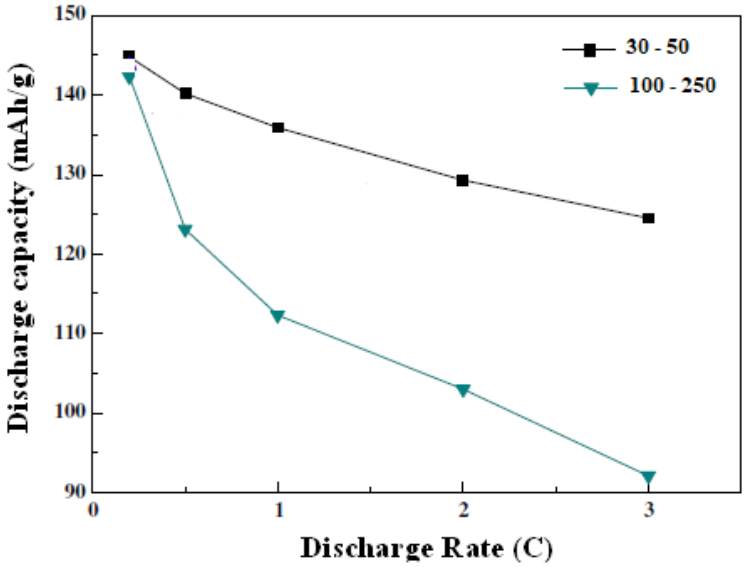

Figure 11. Initial discharge capacities and discharge rate as CNT's diameter varies between 30–50 nm and 100–250 nm.

The results of this study demonstrate that carbon nanotubes possess superior thermal conductivity, hardness, and tensile strength compared to carbon black, while exhibiting comparable electrical resistivity. These findings are consistent with established material property data and confirm the potential of CNTs as high-performance conductive additives.

4. Conclusions

This research presented a comprehensive analysis of carbon nanotubes (CNTs) as conductive additives for $LiNi_{0.5}Co_{0.2}Mn_{0.3}O_2$ (NMC) cathodes. Using Ansys Granta (CES EduPack 2024 R2) software, a systematic comparison of key material properties—including hardness, tensile strength, thermal conductivity, and electrical resistivity—demonstrated the clear superiority of CNTs over conventional carbon black.

The study further investigated the influence of CNT synthesis parameters on electrochemical performance. Multi-walled carbon nanotubes (MWCNTs) derived from a methane precursor exhibited superior performance as conductive additives compared to those from natural gas, which is attributed to their lower electrical resistance and higher crystallinity.

Furthermore, the diameter of the CNTs was found to be a critical factor. MWCNTs with smaller diameters (30–50 nm) significantly enhanced the high-rate capability of the composite cathode. This is due to their higher specific surface area, which provides more charge transport pathways and improves reaction kinetics.

Based on these findings, this study recommends incorporating a minimum of 3 wt% of MWCNTs with a diameter of 30–50 nm to fully exploit the performance of NMC cathodes, particularly under high charge/discharge rates.

Acknowledgments

We would like to thank Fordland Engineering and services for their assistance on the experimental analysis.

Author Contributions

F.N.O.: Conceptualization, Formal Analysis, Investigation, Methodology, Software, Validation, Visualization, Writing—original draft, Writing—review & editing; S.C.N.: Data curation, Formal Analysis, Investigation, Project Administration, Supervision; A.C.O.: Formal Analysis, Investigation, Project Administration, Supervision, Software.

Ethics Statement

Not applicable.

Informed Consent Statement

Not applicable.

Data Availability Statement

The data is available from the corresponding author upon request.

Funding

There was no financial grant in the course of this research and publication.

Declaration of Competing Interest

The authors declare that they have no known competing financial interests or personal relationships that could have appeared to influence the work reported in this paper.

References

1. Chen X, Yang W, Zhang Y. Advanced Electrode Materials for Lithium-ion Battery: Silicon-based Anodes and Co-less-Ni-rich Cathodes. *J. Phys.* **2021**, *2133*, 012003. doi:10.1088/1742-6596/2133/1/012003.
2. Mauger A, Julien CM. Olivine Positive Electrodes for Li-Ion Batteries: Status and Perspectives. *Batteries* **2018**, *4*, 39. doi:10.3390/batteries4030039.
3. Gorji P, Ghahramani M, Haghighi-Yazdi M. The electrochemical performance of $LiFePO_4$ electrodes based on polyurethane binder and carbon fiber current collector for lithium-ion batteries. *J. Energy Storage* **2024**, *99*, 113249. doi:10.1016/j.est.2024.113249.
4. Li J, Peng Y, Wang Q, Liu H. Status and Prospects of Research on Lithium-Ion Battery Parameter Identification. *Batteries* **2024**, *10*, 194. doi:10.3390/batteries10060194.
5. Li Y, Zhao P, Shen B. A review of new technologies for lithium-ion battery treatment. *Sci. Total Environ.* **2024**, *951*, 175459. doi:10.1016/j.scitotenv.2024.175459.
6. Wong KW, Chow WK. Principle for the Working of the Lithium Ion Battery. *J. Mod. Phys.* **2020**, *11*, 1743–1750. doi:10.4236/jmp.2020.1111107.
7. Hou D, Yang T. A reactive molecular dynamics study of graphene oxide sheets in different saturated states: Structure, reactivity and mechanical properties. *Phys. Chem. Chem. Phys.* **2018**, *20*, 11053–11066. doi:10.1039/C8CP00813B.
8. Lobato-Peralta DR, Okoye PU, Alegre C. A review on carbon materials for electrochemical energy storage applications: State of the art, implementation, and synergy with metallic compounds for supercapacitor and battery electrodes. *J. Power Sources* **2024**, *617*, 235140. doi:10.1016/j.jpowsour.2024.235140.
9. Miao Y, Hynan P, von Jouanne A, Yokochi A. Current Li-Ion Battery Technologies in Electric Vehicles and Opportunities for Advancements. *Energies* **2019**, *12*, 1074. doi:10.3390/en12061074.
10. Grey CP, Hall DS. Hall Prospects for lithium-ion batteries and beyond—A 2030 vision. *Nat. Commun.* **2020**, *11*, 6279. doi:10.1038/s41467-020-19991-4.
11. Dan DT. Empowering the Future: Exploring the Construction and Characteristics of Lithium-Ion Batteries. *Adv. Chem. Eng. Sci.* **2024**, *14*, 84–111. doi:10.4236/aces.2024.142006.
12. Salunkhe TT, Kim IT. Expanded Graphite as a Superior Anion Host Carrying High Output Voltage (4.62 V) and High Energy Density for Lithium Dual-Ion Batteries. *Micromachines* **2024**, *15*, 1324. doi:10.3390/mi15111324.
13. Yamada A. High-Voltage Polyanion Positive Electrode Materials. *Molecules* **2021**, *26*, 5143. doi:10.3390/molecules26175143.
14. Choi JH, Choi S, Embleton TJ, Ko K, Saqib KS, Ali J, et al. The Effect of Conductive Additive Morphology and Crystallinity on the Electrochemical Performance of Ni-Rich Cathodes for Sulfide All-Solid-State Lithium-Ion Batteries. *Nanomaterials* **2023**, *13*, 3065. doi:10.3390/nano13233065.
15. Saneifar H, Delaporte N, Zaghib K, Belanger D. Functionalization of the carbon additive of a high-voltage Li-ion cathode. *J. Mater. Chem. A* **2019**, *7*, 1585–1597. doi:10.1039/C8TA07236A.
16. Lee YK. The Effect of Active Material, Conductive Additives, and Binder in a Cathode Composite Electrode on Battery Performance. *Energies* **2019**, *12*, 658. doi:10.3390/en12040658.
17. Capron O, Gopalakrishnan R, Jaguemont J. On the Ageing of High Energy Lithium-Ion Batteries-Comprehensive Electrochemical Diffusivity Studies of Harvested Nickel Manganese Cobalt Electrodes. *Materials* **2018**, *11*, 176. doi:10.3390/ma11020176.
18. Kwon NH, Mouck-Makanda D, Fromm KM. A Review: Carbon Additives in $LiMnPO_4$- and $LiCoO_2$-Based Cathode Composites for Lithium Ion Batteries. *Batteries* **2018**, *4*, 50. doi:10.3390/batteries4040050.
19. Zhou L, Ying H, Han T, Song Y, Yang G, Li L. Carbon-Based Modification Materials for Lithium-ion Battery Cathodes: Advances and Perspectives. *Front. Chem*. **2022**, *10*, 914930. doi:10.3389/fchem.2022.914930.

20. Liu S, Zeng X, Liu D, Wang S, Zhang L, Zhao R, et al. Understanding the Conductive Carbon Additive on Electrode/Electrolyte Interface Formation in Lithium-Ion Batteries via *in situ* Scanning Electrochemical Microscopy. *Front. Chem.* **2020**, *8*, 114. doi:10.3389/fchem.2020.00114.
21. Pérez-Mayoral E, Matos I, Bernardo M, Fonseca LM. New and Advanced Porous Carbon Materials in Fine Chemical Synthesis. Emerging Precursors of Porous Carbons. *Catalysts* **2019**, *9*, 133. doi:10.3390/catal9020133.
22. Hari Prasad PM, Malavika G, Pillai A, Sadan S, Pillai ZS. Emerging organic electrode materials for sustainable batteries. *NPG Asia Mater.* **2024**, *16*, 37. doi:10.1038/s41427-024-00557-5.
23. Michalska M, Buchberger DA, Jasiński JB, Thapa AK, Jain A. Surface Modification of Nanocrystalline $LiMn_2O_4$ Using Graphene Oxide Flakes. *Materials* **2021**, *14*, 4134. doi:10.3390/ma14154134.
24. Kunicky D, Chladil L, Vanysek P. Recent Progress in High-Voltage Cathode Materials for Lithium-Ion Batteries. *ECS Trans.* **2020**, *99*, 17. doi:10.1149/09901.0017ecst.
25. Gribble DA, McCulfor E, Li Z, Parekh M, Pol VG. Enhanced capacity and thermal safety of lithium-ion battery graphite anodes with conductive binder. *J. Power Sources* **2023**, *553*, 232204. doi:10.1016/j.jpowsour.2022.232204.
26. Goodenough JB. How we made the Li-ion rechargeable battery. *Nat. Electron.* **2018**, *1*, 204. doi:10.1038/s41928-018-0048-6.
27. Huang Y, Lin YC, Jenkins DM, Chernova NA, Chung Y, Radhakrishnan B, et al. Thermal stability and reactivity of cathode materials for Li-ion batteries. *ACS Appl. Mater. Interfaces* **2016**, *8*, 7013–7021. doi:10.1021/acsami.5b12081.
28. Zhang G, Zhu Y, Lv S, Wang Z, Gao P. Enhanced electrochemical performance of $LiNiO_2$ cathode material by precursor preoxidation for lithium-ion batteries. *J. Alloys Compd.* **2023**, *953*, 170134. doi:10.1016/j.jallcom.2023.170134.
29. Yang H, Savory CN, Morgan BJ, Scanlon DO, Skelton JM, Walsh A. Chemical Trends in the Lattice Thermal Conductivity of Li(Ni, Mn, Co)O_2 (NMC) Battery Cathodes. *Chem. Mater*. **2020**, *32*, 7542–7550. doi:10.26434/chemrxiv.12320033.
30. Denoyelle Q, Bourgeois L, Tison Y, Martinez H, Carlier D, Boulineau A, et al. Thermal Stability of Li_xCoO_2 Electrodes for All-Solid-State Secondary Batteries Operating at High-Temperature. *ECS Meet. Abstr.* **2020**, *237*, 423. doi:10.1149/MA2020-012423mtgabs.
31. Kaneko K, Li M, Noda S. Appropriate properties of carbon nanotubes for the three-dimensional current collector in lithium-ion batteries. *Carbon Trends* **2023**, *10*, 100245. doi:10.1016/j.cartre.2022.100245.
32. Okoye CO, Jones I, Zhu M, Zhang Z, Zhang D. Manufacturing of carbon black from spent tyre pyrolysis oil—A literature review. *J. Clean. Prod.* **2021**, *279*, 123336. doi:10.1016/j.jclepro.2020.123336.
33. Gotcu P, Pfleging W, Smyrek P, Seifert HJ. Thermal behaviour of $LixMeO_2$ (Me = Co or Ni + Mn + Co) cathode materials. *Phys. Chem. Chem. Phys.* **2017**, *19*, 11920–11930. doi:10.1039/C7CP00513J.
34. Peng J, Grayson M, Snyder GJ. What makes a material bendable? A thickness-dependent metric for bendability, malleability, ductility. *Matter* **2021**, *4*, 2694–2696. doi:10.1016/j.matt.2021.07.015.
35. Ulianov C, Önder A, Peng Q. Analysis and selection of materials for the design of lightweight railway vehicles. *Mater. Sci. Eng.* **2018**, *292*, 012072. doi:10.1088/1757-899X/292/1/012072.
36. Tyler K, Stefani N, Mohee L. Teaching Engineering Design with Materials Selection and Simulation through Case Studies: A Work in Progress. In Proceedings of the 2022 ASEE Annual Conference, Minneapolis, MN, USA, 26–29 June 2022; pp. 1–13.
37. Chen B, Zhang Z, Xiao M, Wang S, Huang S, Han D, et al. Polymeric Binders Used in Lithium Ion Batteries: Actualities, Strategies and Trends. *ChemElectroChem* **2024**, *11*, e202300651. doi:10.1002/celc.202300651.
38. Miranda B, Goren A, Costa CM. Theoretical simulation of the optimal relation between active material, binder and conductive additive for lithium-ion battery cathodes. *Energy* **2019**, *172*, 68–78. doi:10.1016/j.energy.2019.01.122.